ELSEVIER

Clinical Biomechanics 15 (2000) 718–725

CLINICAL BIOMECHANICS

www.elsevier.com/locate/clinbiomech

Load-bearing and stress analysis of the human spine under a novel wrapping compression loading

A. Shirazi-Adl [a,*], M. Parnianpour [b]

[a] *Division of Applied Mechanics, Department of Mechanical Engineering, Ecole Polytechnique, P.O. Box 6079, Station Centre-cille, Montreal, Quebec, Canada H3C 3A7*

[b] *IWSE Department, The Ohio State University, Columbus, OH, USA*

Received 27 April 2000; accepted 13 July 2000

Abstract

Objective. To examine biomechanics of the human spine under a novel compression loading that follows the curvature of the spine.

Design. The detailed response of the spine is predicted and compared under various types of compression loading at different postures.

Background. The posture and loading configuration could be so adjusted as to increase load-bearing capacity and stability of the spine in compression while minimizing the muscle activity and risk of tissue injury.

Methods. The nonlinear finite element formulation of wrapping elements sliding over solid body edges is developed and used to study the load-bearing capacity of simplified beam-rigid body thoracolumbar (T1–S1) and lumbosacral (L1–S1) spines under a wrapping compression force. The load-bearing and stress analysis of a detailed model of the lumbar spine, L1–S1, is also investigated under five wrapping loads resulting in differential compression forces at various levels. Follower load at L1, axially fixed compression at L1, and combined axially fixed compression and moments load are also considered for comparison. For the detailed model, the effect of changes in the position of wrapping elements and in the lumbar curvature on results are considered.

Results. The idealized wrapping loading stiffens the spine, allowing it to carry very large compression loads without hypermobility. It diminishes local segmental shear forces and moments as well as tissue stresses.

Conclusions. In comparison to fixed axial compression, the compression loading by wrapping elements that follow the spinal curvatures increases the load-bearing capacity in compression and provides a greater margin of safety against both instability and tissue injury.

Relevance

These findings suggest a plausible mechanism in which postural changes and muscle activation patterns could be exploited to yield a loading configuration somewhat similar to that of the wrapping loading, i.e., the net reaction force at various levels passes through discs nearly normal to their mid-height plane. To alleviate hypermobility in compression, the wrapping loading could also allow for the application of meaningful compression loads in experimental as well as model studies of the multi-segmental spinal biomechanics.

1. Introduction

Similar to an imperfect column under axial compression, the human ligamentous thoracolumbar and lumbar spines devoid of musculature exhibit hypermobility or functionally excessive displacements under compression loads as low as only ~20 and ~80 N, respectively [1–4]. These compression loads are, however, only a small fraction of those experienced by the human spine during the activities of daily living. Mechanisms by which compressive loads during regular physiological activities and heavy manual material handling tasks can be tolerated by the human spinal column without abnormal motions, though the subject of many studies (e.g., [5–9]), remain yet to be identified. In our recent in vivo and finite element model studies, the compression load-bearing capacity of the human spine has been demonstrated to be markedly influenced

* Corresponding author.
E-mail address: abshir@meca.polymtl.ca (A. Shirazi-Adl).

0268-0033/00/$ - see front matter
PII: S0268-0033(00)00045-0

by changes in the pelvic tilt, lumbar curvature, T1 positioning, load distribution/position, and small muscle activity [4,10–13].

It is plausible to conclude, based on previous works, that the posture, at a given task and load level, is so adjusted as to produce a loading configuration that can be maintained by the passive spinal column with minimal physiological displacements and a sufficient margin of safety against instability while minimizing the muscle activation level. By analogy of the spinal column to the masonry arch, Aspden [5] proposed loading configurations the resultant forces of which lie entirely within the cross-section of the spine all along the column, thus calculating the required muscle activities and intra-abdominal pressure. Gracovetsky et al. [14] suggested, for a given task, the existence of a unique lumbar posture that minimizes and equalizes the compressive stress within the spine requiring minimum muscular activity. Due to the inherent instability in compression and absence of stabilizing mechanisms, previous in vitro studies on unconstrained spinal multi-motion segments were not able to consider compression loads of meaningful magnitudes. In a search to alleviate this shortcoming, Patwardhan et al. [15] have recently developed a novel load application system in which the compression force follows the curvature of the lumbar spine by pulling two cables on both sides of the spine guided to follow the displacements of vertebral bodies. In this manner, they were able to apply compression loads beyond 1000 N on the lumbar spine cadaver specimens with no sign of instability. This observation was confirmed in various lordotic, neutral, and flexed postures.

In an earlier study, we have developed and validated the nonlinear finite element formulation of a novel uniaxial element that, in between the insertion points, wraps around (i.e., comes into contact with) prescribed spatial target edges on a number of deformable or rigid bodies [16]. This formulation was initially intended for the simulation of the medial collateral ligament in our model studies of the human knee joint under different loads [17,18]. In the current study, the developed wrapping elements are employed to apply compression loads on the spine in such a manner as to continuously, during deformation, remain perpendicular (or nearly perpendicular) to the disc mid-plane at different levels, thus minimizing local shear and moment loads. Both simplified beam-rigid body lumbosacral, L1–S1, and thoracolumbar, T1–S1, models are used. The wrapping compression loading is then used to perform stress analysis of a detailed L1–S1 model [19,20] under up to 2800 N compression applied with a single wrapping element (i.e., constant compression along the lumbar levels) or with five wrapping elements resulting in differential compression forces along the lumbar discs.

It is hypothesized that the spinal compression load-bearing capacity substantially increases when the compression loads are applied through wrapping elements that follow the spinal curvature (i.e., wrapping loading). Moreover, such loading configuration, under identical segmental rotations and applied compression, will significantly alter the state of stress in various tissues, resulting in a greater margin of safety against tissue injury as compared with that evaluated under axially fixed compression loading.

2. Methods

2.1. Finite element models

2.1.1. Detailed L1–S1 model

The detailed lumbosacral model, L1–S1, is described elsewhere [19–21] and is only briefly presented here. Computer-assisted tomography of a cadaver specimen of a 65-year-old man and finite element mesh generation are merged to construct a detailed finite element model of the entire L1–S1 ligamentous lumbar spine (Fig. 1).

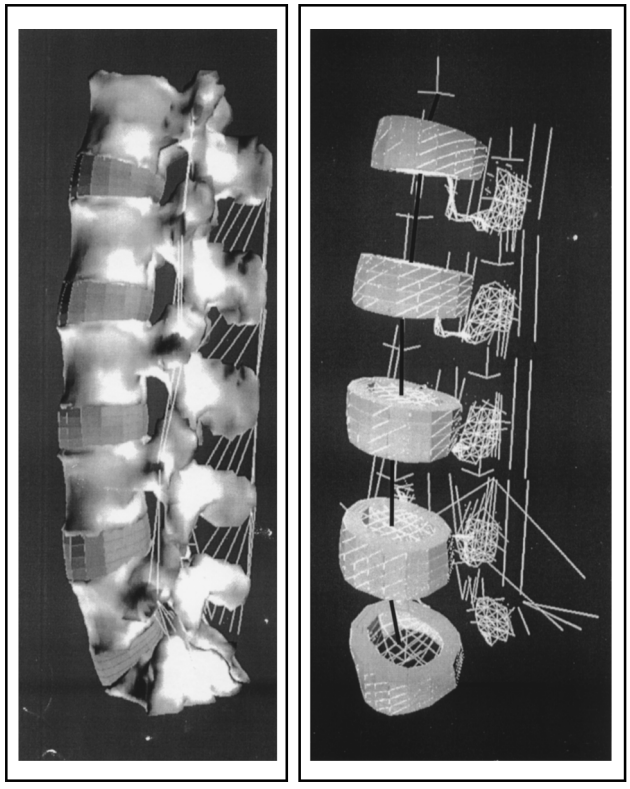

Fig. 1. Lateral views of the detailed finite element model of the entire lumbar spine, L1–S1. Left: view of segments with vertebral bodies, discs and ligaments; Right: lateral view showing discs, ligaments and superior articular surfaces of facets, the L1 vertebra at the top and the S1 at the bottom. Each bony vertebra is modeled by two separate rigid bodies attached by two deformable beams oriented along its pedicles. A single wrapping element is also shown passing through vertebral end-plate centers (guided to slide on predifined target edges attached to vertebral end-plates, not shown).

The model includes six vertebrae (L1 to S1), five intervertebral discs, ten sets of superior–inferior articulating facet surfaces (two at each segmental level), and a number of ligaments (supraspinous, interspinous, posterior/anterior longitudinal, flavum, transverse, capsular, iliolumbar, and fascia). Each vertebra is modeled as two independent rigid bodies, one for the anterior body and the other for the posterior bony elements. These two are attached by two deformable beam elements oriented along the pedicles. The global *xyz* coordinate system is set with the *z*-axis (axial direction) perpendicular to the mid-plane of the L3–L4 disc, and the *x*- and *y*-axes being in the sagittal (positive toward posterior) and lateral (positive toward right) directions, respectively. The geometry of the lumbar spine, including its facet surfaces, is not symmetric about the sagittal plane [19].

At each segmental level, the disc annulus is modeled as a composite of an isotropic annulus bulk reinforced by membrane collagen fibers and the nucleus as a fluid-filled cavity with the possibility to prescribe changes in the fluid content or pressure. A slope of 27° is assumed for the collagen fibers of all discs. The articulation at facet joints is formulated as a large displacement frictionless contact problem. The rigid bodies (i.e., bony structures) are attached to deformable elements and contain fluid-filled cavities. They could also articulate with each other. The beam elements attaching the rigid bodies use a convective formulation allowing for large displacements. The nonlinear material and structural properties used for different regions (i.e., disc fibers and ligaments) are similar to those reported in our earlier studies. The presence of articular cartilage layers on facet surfaces, not explicitly discretized in the model, is simulated by gap elements with no resistance in tension and a stiffening resistance in compression (moduli of 75 and 150 MPa). Moreover, a gap limit of 1.25 mm is assumed, below which distance the adjacent bodies come into contact with each other and transfer load.

In this study, the caudal vertebra S1 is fixed while the remaining vertebrae L1–L5 are unconstrained. Axially fixed compression loads of up to 2800 N are incrementally applied at all L1–L5 vertebral centers (80% at the L1 and the rest evenly distributed among remaining L2–L5 vertebrae to account for differential compression loads along the lumbar spine, see [10]). The original lordosis of ~46° (i.e., the angle between lower L1 and upper S1 bony end-plate surfaces) is either left constrained or decreased by up to 38° (i.e., flexion). The flattening of the lordosis is prescribed at different levels by different values, that is, under 2800 N axial compression, the lordosis is incrementally decreased by up to 4°, 7°, 9°, 11° and 7° at L1 to L5 vertebrae, respectively, resulting in a total flattening of 38°. The foregoing cases simulate different flexion angles among lumbar vertebral bodies and are taken so as to cover a whole range of possibilities based on the results of kinematics measurements during voluntary trunk forward bending and lifting tasks reported in the literature (see [10]). The lateral rotations of the L1–L5 vertebral bodies are constrained in cases where sagittal rotations are prescribed. For these cases, the required sagittal/lateral moments at various segmental levels are evaluated at each load increment. These moments are likely generated by changes in the posture (i.e., position of the applied loads) and muscle activation (see Table 1).

2.1.2. Simplified L1–S1 and T1–S1 models

A simplified beam-rigid body model of the L1–S1 (lumbar region of Fig. 2) is also used for the study of the effect of various loading configurations (i.e., axially fixed compression with and without prescribed rotations, follower compression load, and wrapping compression load) on results. The model consists of six rigid bodies representing L1–S1 vertebrae and five deformable beams representing discs (see [3] for more details; see also Table 1 for a list of loading cases considered). A similar beam-rigid body model of the thoracolumbar spine, T1–S1, (Fig. 2) is also used under wrapping compression loading with 18 rigid bodies for vertebrae and 17 deformable beams for intervertebral discs (see [4] for more details). The analysis of the L1–S1 model under follower load is carried out using the Abaqus FE program while the remaining cases are analyzed using an in-house FE program.

Table 1
List of various compression loading cases

FE model	Axially fixed	Follower	Wrapping
Detailed L1–S1	At all L1–L5 levels with constraints on rotations (i.e., combined)		1 element only, with no constraint on rotations
			5 elements, with/without constraints on rotations
			5 elements, with 2 or 3 mm posterior shift in target contact edges (no constraint on rotations)
Simplified L1–S1	At L1 only, with/without constraint on rotations	At L1 only	1 element only
Simplified T1–S1			1 element only

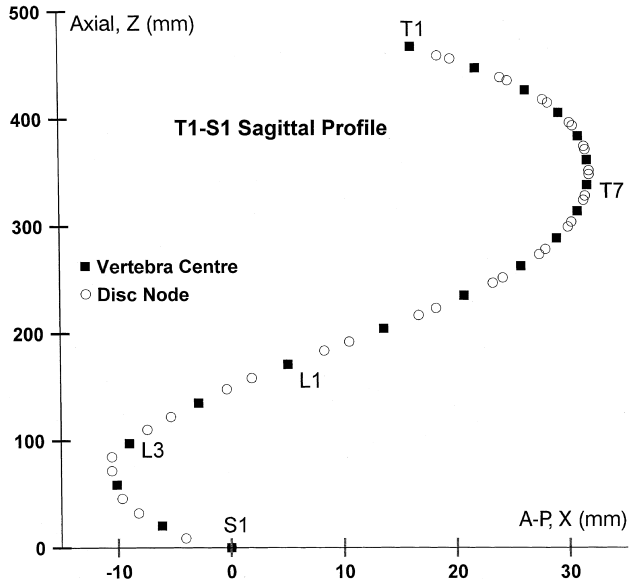

Fig. 2. Sagittal profile of the simplified beam-rigid body thoracolumbar model, T1–S1. Eighteen vertebrae are modeled by rigid bodies, while the segmental stiffnesses are presented by 17 deformable beam elements at each disc level. The lower L1–S1 portion of this model presents the simplified lumbosacral, L1–S1, model.

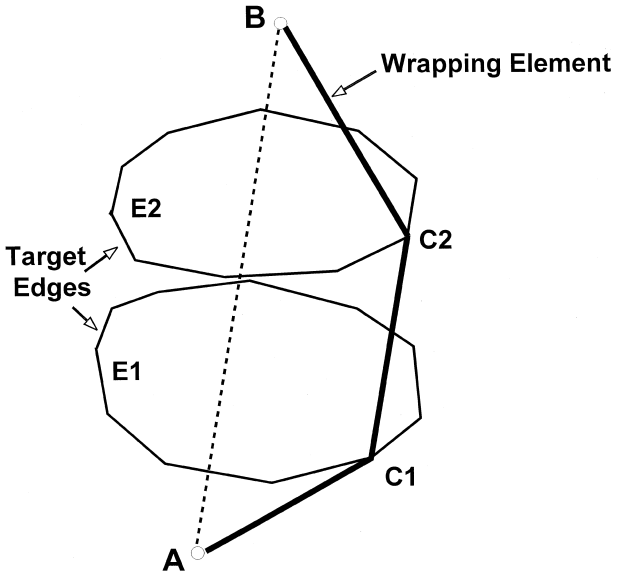

Fig. 3. An example of a wrapping element with insertion points A and B sliding on two general target edges E1 and E2 at contact points C1 and C2, respectively. The element cannot be formulated as either a straight element between insertion points (dashed line A–B) or as a collection of three individual straight elements(A–C1, C1–C2, and C2–B). The target edges and/or contact points could change during the course of loading (as in a general contact algorithm).

2.2. Wrapping elements/loading

The details of the nonlinear finite element formulation for the wrapping element and its validation are given elsewhere [16] and are described here only briefly. The simulation of wrapping elements sliding frictionless over solid bodies, at each increment of the analysis, is initially based on the identification of those target body edges that could articulate with any wrapping element and, as such, requires, therefore, a contact algorithm (Fig. 3). It is followed by the determination of a contact point on each potential target edge over which the wrapping element slides, resulting in the complete definition of a wrapping element attaching these sliding contact points to its insertion end-points. In this manner, each wrapping element exactly simulates a cable passing through vertebral end-plate centers. Once the contact points (a total of, say, q points) are determined, the incremental tangent stiffness of the whole wrapping element with $(q+1)$ straight sub-elements and $3\times(q+2)$ degrees of freedom (for a three-dimensional analysis) is developed with cross-coupling between all associated degrees of freedom, on both insertion and contact points. The $3\times(q+2)$ by $3\times(q+2)$ wrapping stiffness matrix, therefore, depends on the instantaneous geometry of its sub-elements, the rigidity of the element itself, and the tensile force in the element which, at each increment, remains constant in all sub-elements (i.e., neglecting friction at contact points). In the absence of any contact point, this matrix reduces to the conventional, nonlinear 6×6 matrix of a two-node truss element. The compression load is applied through each wrapping element by inserting the upper end of the element into a vertebral center and the lower end on a mobile support free to move in a direction, say X, while applying the incrementally increasing tensile load at this end in the same direction, X. As the applied load increases, the wrapping elements slide over different target edges and likely change target edges and/or contact points from an increment to the next.

2.2.1. Detailed L1–S1 model

The articulating target edges on the vertebral end-plates are so prescribed as to guide the wrapping elements through approximately the geometric centers of end-plates (Figs. 1 and 4). In order to evaluate the influence of the positioning of the wrapping elements on results, additional cases are subsequently analyzed with the target edges of this reference case modified by a posterior shift of 2 or 3 mm. The total compression force of 2800 N is applied by five wrapping elements resulting in 80% of the compression on L1 increasing distally to 100% on L5 (i.e., 80% of load applied on the wrapping element attached to L1 and 5% on the remaining elements attached to L2, L3, L4, or L5). In the detailed L1–S1 model, the sagittal rotations at different vertebral levels remain either unconstrained or prescribed to undergo no change (no rotations) or a maximum total of 38° lumbar flexion. An additional unconstrained L1–S1 model with a single wrapping element carrying up to 2800 N compression is also studied. The lateral

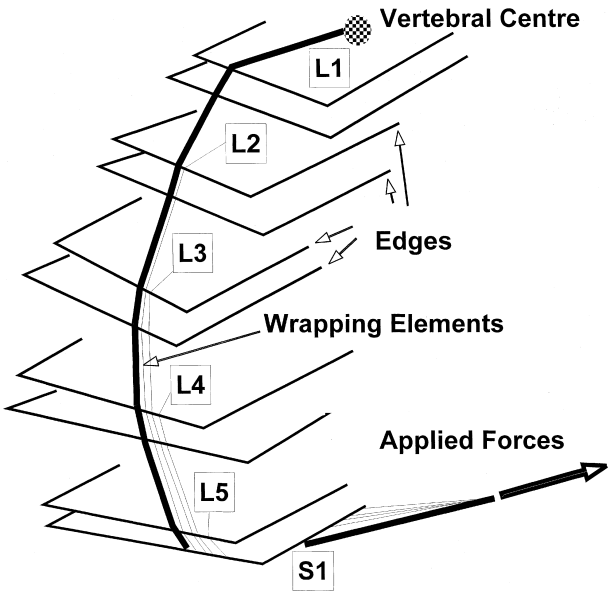

Fig. 4. A schematic representation of five wrapping elements sliding on bony end-plate edges of the detailed lumbosacral model. The upper end of each wrapping element is attached to a vertebral centre while its lower end is loaded at the bottom (see Fig. 1 for the one attached to the L1 vertebra).

rotations are always constrained. Table 1 lists the various cases considered.

2.2.2. Simplified L1–S1 and T1–S1 models

The target edges on both end-plates of each vertebra are selected in such a manner as to have the end nodal points of beams representing discs as sliding contact points. In this case, a wrapping element continuously follows the intervertebral discs (i.e., deformable beam elements) and, hence, the spinal curvature, remaining precisely normal to the disc mid-planes. Under the incrementally-increasing applied wrapping load, the sagittal and lateral rotations at different vertebral levels are left unconstrained.

3. Results

In the simplified L1–S1 model (Figs. 5 and 6), large displacements (i.e., hypermobility) is noted under an axially fixed compression load of ~100 N applied at L1. The response noticeably stiffens under a nonconservative follower compression load that follows the rotation of L1, while nearly no horizontal translations are predicted when the compression is applied by a wrapping element. In this case of wrapping loading, segmental rotations in all directions remain nil even though they are left unconstrained in the model. Moreover, each disc is subjected to a pure state of compression loading with absolutely no local shear forces or moments. A similar stiffening effect is computed under axial compression at

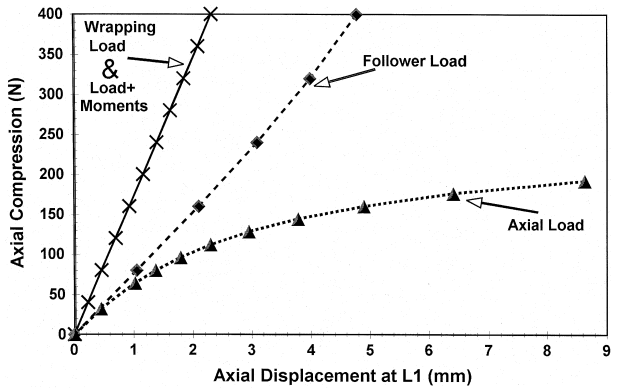

Fig. 5. Predicted variation of the L1 axial translation versus applied compression for the simplified lumbar model under various loading configurations. For the wrapping case, only one element is considered, resulting in a constant compression along the lumbar spine. In the combined load + moment case, the sagittal/lateral rotations at all levels are constrained under an axial compression at the L1 and the required moments are calculated. The follower load case presents a single load, initially axial, that follows the rotation at L1.

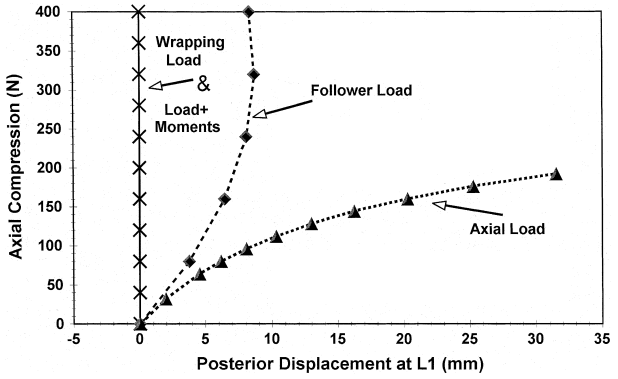

Fig. 6. Predicted variation of the L1 sagittal translation versus applied compression for the simplified lumbar model under various loading configurations. For the wrapping case, only one element is considered, resulting in a constant compression along the lumbar spine. In the combined load + moment case, the sagittal/lateral rotations at all levels are constrained under an axial compression at L1 and the required moments are calculated. The follower load case presents a single load, initially axial, that follows the rotation at L1.

L1 when segmental rotations are constrained, i.e., in the case of combined compression and moments loading. In this case, sagittal moments (+ve: flexion; in N m) of 1.7, 2.8, 1.7, −0.6, −2.7 and −0.8 are required for the constraint on sagittal rotation at the L1 down to S1 vertebrae, respectively, under 400 N axial compression at L1. In these latter two wrapping and combined loading conditions, therefore, the lumbar curvature remains unchanged during the loading. Larger compression loads could also have been maintained for these two cases. Similarly, for the simplified thoracolumbar spine (Fig. 7), T1–S1, the compression loading of the system by a single wrapping element yields a stable response

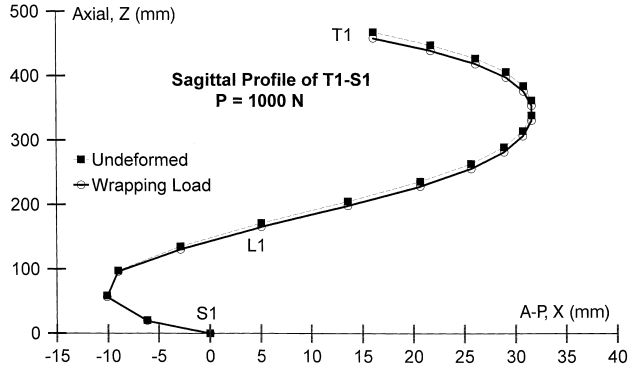

Fig. 7. Initial, undeformed and final, deformed sagittal profiles of the simplified thoracolumbar model under 1000 N compression applied by a single wrapping element. The model is completely unconstrained except a full fixation at the base, S1. T1 and L1 translate axially by 8.9 and 5.8 mm, respectively, under the load of 1000 N. The wrapping loading generates no segmental rotations and no shear forces/moments at all levels.

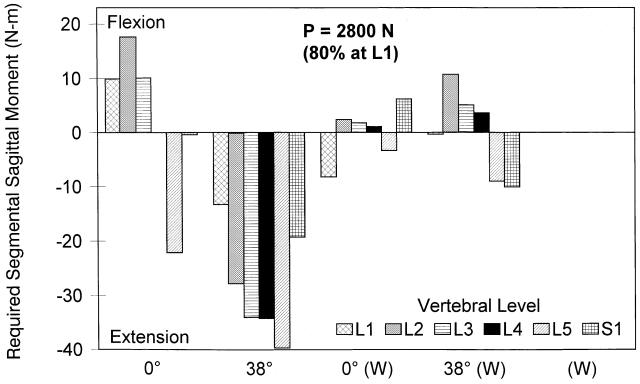

Fig. 8. Required sagittal moment (+ve: flexion) at various vertebral levels in the detailed L1–S1 model under 2800 N compression distributed at all levels for two loading cases: axially fixed compression loading constrained at total flexion angles of 0° or 38°, and for wrapping loading (*W*) with five wrapping elements, constrained at 0°, 38° or left unconstrained (for which no moments are needed). These moments are required for the prescribed segmental rotations.

with no rotations, shear forces and moments at different levels irrespective of the magnitude of the compression load considered. In contrast, however, the unconstrained T1–S1 model exhibits large displacements under very small axial compression loads of ~30 N [4].

For the detailed L1–S1 model (Fig. 1), the response under the wrapping load is influenced by the position of the wrapping elements. For the reference case, the application of a total of 2800 N by five wrapping elements flattens the unconstrained lumbar spine by 14.5°. This total L1–S1 flexion rotation decreases to 2.3° as the target edges (position of wrapping elements) shift posteriorly by 2 mm and further to an extension rotation of 3.1° (i.e., more lordotic curvature) as the posterior shift in target edges (sliding contact points) increases to 3 mm. One single wrapping compression load of 2800 N at the reference position causes 14.9° flexion at the lumbar spine. The lateral rotation at L1 for these cases remains nearly the same at 4.4° in the right lateral direction. For these unconstrained cases, the system is naturally stable, with no requirement for sagittal or lateral moments to maintain equilibrium at different levels (Fig. 8). In contrast, however, additional moments are required when the segmental rotations are constrained by some prescribed values, either at zero or a total of 38° (Fig. 8). It is, nevertheless, noted that the required equilibrating moments are substantially smaller when the compression loads are applied through wrapping elements than when they are applied as external loads fixed to remain in axial direction.

For identical prescribed changes in the lordosis (0° or 38°), the application of compression load by wrapping elements does not have a noticeable effect on the magnitude of intradiscal pressure at various levels (Fig. 9). It, however, substantially decreases the maximum disc fibre strains occurring in the innermost

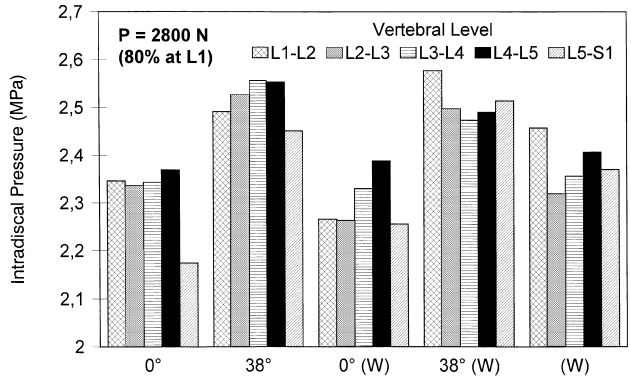

Fig. 9. Computed disc pressure at various levels in the detailed L1–S1 model under 2800 N compression distributed at all levels for two loading cases: axially fixed compression loading constrained at total flexion angles of 0° or 38°, and for wrapping loading (*W*) with five wrapping elements, constrained at 0°, 38° or left unconstrained.

annulus layer at various disc levels, particularly under larger flexion angles (Fig. 10). As for the total facet forces, a large decrease is computed at the distal L5–S1 level under wrapping loadings at smaller flexion angles. Under larger lumbar flexion angles, the facet forces are considerably decreased at all levels when the compression is applied by wrapping elements (Fig. 11). The flattening of the lumbar spine appears to have a decreasing effect on facet forces under wrapping loading – a trend that appears to be in contrast to that under conservative axial compression forces. The posterior shifts in the position of wrapping cables at contact points by 2 or 3 mm result in slightly smaller intradiscal pressures, larger maximum disc fibre strains at distal L3–S1 disc levels, and much larger facet forces at all vertebral levels.

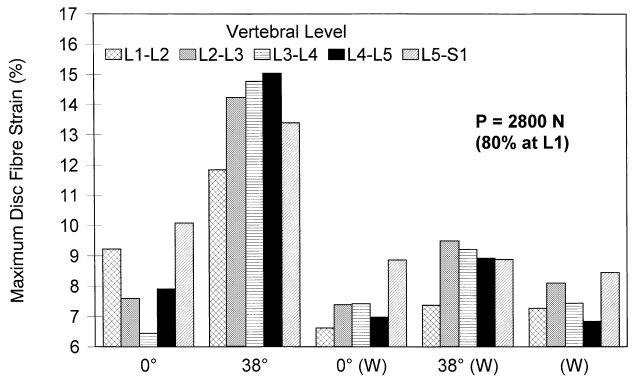

Fig. 10. Computed maximum disc fibre strains at various disc levels in the detailed L1–S1 model under 2800 N compression distributed at all levels for two loading cases: axially fixed compression loading constrained at total flexion angles of 0° or 38° and for wrapping loading (*W*) with five wrapping elements, constrained at 0°, 38° or left unconstrained. In all discs, the maximum fibre strain occurs in the annulus innermost layer in the posterolateral and lateral directions, reducing towards the annulus outermost layer.

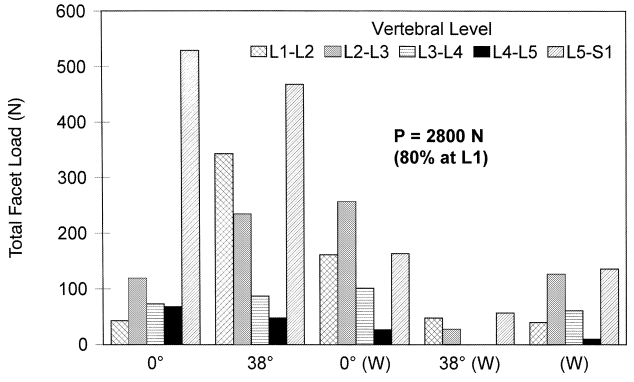

Fig. 11. Computed total facet forces (as simple sum of the left and right facet total resultant forces) at various levels in the detailed L1–S1 model under 2800 N compression distributed at all levels for two loading cases: axially fixed compression loading constrained at total flexion angles of 0° or 38° and for wrapping loading (*W*) with five wrapping elements, constrained at 0°, 38° or left unconstrained. It is to be noted that the facet forces at the left and right facets are not equal due to asymmetry.

4. Discussion

The passive ligamentous human spine, by itself, can carry only a small fraction of the compression loads experienced in activities of daily living and in manual material handling tasks without exhibiting hypermobility. Active muscle exertion could stabilize the spine, allowing it to carry large compression loads while performing various tasks [6–9]. The drawback, however, is that large muscle forces, while able to help maintain the loads and stabilize the system, place greater compression penalty on the spine, thereby reducing the margin of safety by increasing the risk of tissue injury as well as muscle fatigue. Our earlier studies have demonstrated that changes in the lumbar posture, pelvic tilt, T1 positioning, and load distribution/location could act as likely mechanisms to enhance the load-bearing capacity of the system in neutral postures and, hence, reduce the need for greater active muscle contribution [3,4,10–13].

The kinetic redundancy of the human trunk presents a rather insurmountable obstacle in estimating the muscle activation patterns and postural adaptations that allow the maintenance of equilibrium at minimal muscle activation while providing a sufficient margin of safety against instability and tissue injury. The redundancy in the trunk active system can serve in balancing the varying external moments along the spine, actively augmenting the stiffness of the system by adequate activation level, and controlling posture in order to minimize passive tissue stresses and strains. To arrive at an optimal synergy between active and passive components, the direction and location of the net joint reaction force may need to be adjusted and controlled. In the current study, a novel compression loading configuration applied by wrapping elements is modeled that follows the spinal curvature to remain continuously normal to disc mid-height planes. A wrapping element exactly simulates a cable guided to pass through vertebral end-plate centers. It is found that, under identical total compression force and segmental rotations, such idealized wrapping loading configuration markedly diminishes the segmental shear forces and moments as compared with axially fixed compression loading. The tissue stresses and, hence, risk of tissue injury as well as required muscle activation level and, hence, risk of muscle fatigue are also substantially decreased under wrapping loading. These trends suggest, therefore, a plausible mechanism in which changes in the posture and muscle activation are so exploited as to yield an optimal loading configuration somewhat similar to that of the wrapping case. Any impairment in the neuro-musculo-osteoligamentous spine could, if not adequately compensated for, lead to abnormal loading/motions that may predispose the spine to degeneration and disorders.

The predictions of this model study are in accordance with the recent experimental observations of Patwardhan et al. [15], who applied compression loads through guided cables on both sides of vertebrae in a manner identical to our wrapping elements, though these latter ones pass through the vertebral end-plate centers. As in the current study, they noted that, unlike under axially fixed compression load, the ligamentous human lumbar spine is stiff and stable under a compression load applied similar to that formulated in our model studies. This was verified in various lordotic, neutral, and flattened postures where the response depended on the position of the wrapping cables. Such means of applying compression loads would overcome the existing shortcoming in

experimental and model studies, where meaningful compression loads could not be considered due to the inherent lack of adequate system stiffness (i.e., hypermobility).

Finally, a nonlinear finite element of a novel loading configuration using wrapping elements is formulated and applied for the model studies of lumbar and thoracolumbar spines in compression. Such loading maintains the equilibrium and stability of the system under much larger compression loads, while it minimizes tissue stresses and risk of injury as well as muscle activation and risk of muscle fatigue as compared with the case under axially fixed compression loads. The redundancy in the active system and changes in posture could be exploited to yield a loading configuration similar to the wrapping loading in which the shear forces and moments are minimized. Future research on active–passive load distribution and synergy in spinal column accounting for both muscle activation and postural adaptations should identify the relative feasibility of such idealized loading configurations.

Acknowledgements

The work is supported by grants from the Natural Sciences and Engineering Council of Canada (NSERC-Canada) and Institut de Recherche en Santé et Sécurité du Travail du Québec (IRSST-Québec).

References

[1] Crisco JJ, Panjabi M. The intersegmental and multisegmental muscles of the lumbar spine: A biomechanical model comparing lateral stabilizing potential. Spine 1991;16:793–808.
[2] Lucas DB, Bresler B. Stability of the ligamentous spine. Technical report Ser. 11, No. 40. San Francisco: Biomechanics Laboratory, University of California; 1960. p. 1–41.
[3] Shirazi-Adl A, Parnianpour M. Nonlinear response analysis of the human ligamentous lumbar spine in compression: On mechanisms affecting the postural stability. Spine 1993;18:147–58.
[4] Shirazi-Adl A, Parnianpour M. Stabilizing role of moments and pelvic rotation on the human spine in compression. J Biomech Eng 1996;118:26–31.
[5] Aspden RM. The spine as an arch – A new mathematical model. Spine 1989;14:276–84.
[6] Bergmark A. Stability of the lumbar spine: A study in mechanical engineering. Acta Orthop Scand 1989;60(Suppl 230):1–54.
[7] Cholewicki J, Panjabi M, Khachatryan A. Stabilizing function of trunk flexor–extensor muscles around a neutral spine posture. Spine 1997;22:2207–12.
[8] Cholewicki J, Juluru K, McGill SM. Intra-abdominal pressure mechanism for stabilizing the lumbar spine. J Biomech 1999;25:17–28.
[9] Gardner-Morse M, Stokes IAF, Laible JP. Role of muscles in lumbar spine stability in maximum extension efforts. J Orthop Res 1995;31:802–8.
[10] Shirazi-Adl A, Parnianpour M. Effect of changes in lordosis on mechanics of the lumbar spine – Lumbar curvature in lifting. J Spinal Dis 1999;12:436–47.
[11] Shirazi-Adl A, Parnianpour M. Pelvic tilt and lordosis control spinal postural response in compression. In: Transactions of the Orthop Res Soc. CA: Anaheim; 1999. p. 1012.
[12] Kiefer A, Shirazi-Adl A, Parnianpour M. On the stability of human spine in neutral postures. Eur Spine J 1997;6:45–53.
[13] Kiefer A, Shirazi-Adl A, Parnianpour M. Synergy of human spine in neutral postures. Eur Spine J 1998;7:471–9.
[14] Gracovetsky S, Kary M, Pitchen I, Levy S, BenDaid R. The importance of pelvic tilt in reducing compressive stress in the spine during flexion–extension exercises. Spine 1989;14:412–6.
[15] Patwardhan A, Havey RM, Meade KP, Lee B, Dunlap B. A follower load increases the load-carrying capacity of the lumbar spine in compression. Spine 1999;24:1003–9.
[16] Shirazi-Adl A. Nonlinear finite element analysis of wrapping uniaxial elements. Comput Struct 1989;32:119–23.
[17] Bendjaballah MZ, Shirazi-Adl A, Zukor DJ. Biomechanics of the human knee joint in compression: Reconstruction, mesh generation and finite element analysis. The Knee 1995;2:69–79.
[18] Bendjaballah MZ, Shirazi-Adl A, Zukor DJ. Biomechanical response of the human knee joint under anterior–posterior forces. Clin Biomech 1998;13:625–33.
[19] Shirazi-Adl A. Nonlinear stress analysis of the whole lumbar spine in torsion – Mechanics of facet articulation. J Biomech 1994;27:289–99.
[20] Shirazi-Adl A. Biomechanics of the lumbar spine in sagittal/lateral moments. Spine 1994;19:2407–14.
[21] Breau C, Shirazi-Adl A, deGuise J. Reconstruction of a human ligamentous lumbar spine using CT images – A three-dimensional finite element mesh generation. Ann Biomed Eng 1990;19:291–302.